DOI: 10.1002/arch.21527

RESEARCH ARTICLE

WILEY Archives of INSECT BIOCHEMISTRY AND PHYSIOLOGY

RNA interference-mediated knockdown of eye coloration genes in the western tarnished plant bug (*Lygus hesperus* Knight)

Colin S. Brent* | **J. Joe Hull***

USDA-ARS Arid Land Agricultural Center, Maricopa, Arizona

Correspondence
Colin S. Bren, USDA-ARS Arid Land Agricultural Center, Maricopa, AZ 85138.
Email: colin.brent@ars.usda.gov

Funding information
Cotton Incorporated, Grant/Award Number: 16–410

Abstract

Insect eye coloration arises from the accumulation of various pigments. A number of genes that function in the biosynthesis (*vermilion*, *cinnabar*, and *cardinal*) and importation (*karmoisin*, *white*, *scarlet*, and *brown*) of these pigments, and their precursors, have been identified in diverse species and used as markers for transgenesis and gene editing. To examine their suitability as visible markers in *Lygus hesperus* Knight (western tarnished plant bug), transcriptomic data were screened for sequences exhibiting homology with the *Drosophila melanogaster* proteins. Complete open reading frames encoding putative homologs for all seven genes were identified. Bioinformatic-based sequence and phylogenetic analyses supported initial annotations as eye coloration genes. Consistent with their proposed role, each of the genes was expressed in adult heads as well as throughout nymphal and adult development. Adult eyes of those injected with double-stranded RNAs (dsRNAs) for *karmoisin*, *vermilion*, *cinnabar*, *cardinal*, and *scarlet* were characterized by a red band along the medial margin extending from the rostral terminus to the antenna. In contrast, eyes of insects injected with dsRNAs for both *white* and *brown* were a uniform light brown. *White* knockdown also produced cuticular and behavioral defects. Based on its expression profile and robust visible phenotype, *cardinal* would likely prove to be the most suitable marker for developing gene editing methods in *Lygus* species.

*Brent and Hull are joint first author.

KEYWORDS
eye color, *Lygus hesperus*, ommochrome, pteridine, RNAi

1 | INTRODUCTION

Insect eye coloration is largely dependent on the accumulation of two classes of pigments within distinct membrane-bound organelles of eye pigment cells (Lloyd, Ramaswami, & Krämer, 1998). Tryptophan-derived ommochromes are the lone pigmentation source in a number of insects (Beard, Benedict, Primus, Finnerty, & Collins, 1995; Dustmann, 1968; Lorenzen, Brown, Denell, & Beeman, 2002; Moraes, Pimentel, Rodrigues, & Mello, 2005; Tatematsu et al., 2011). In contrast, a combination of ommochromes and guanine-derived pteridine pigments contribute to eye coloring in a more limited number of species including *Drosophila melanogaster* (Summers, Howells, & Pyliotis, 1982), *Schistocerca americana* (Dong & Friedrich, 2005), and *Nilaparvata lugens* (Liu et al., 2013). A number of genetic loci initially found to influence Drosophila eye coloration have since been shown to correspond to genes encoding biosynthetic pathway enzymes, ATP-binding cassette (ABC) transporters, and vesicular transport proteins (Lloyd et al., 1998). Given the ease of visual screening, eye color mutations have been used as genetic markers for germ-line transformation (Cornel, Benedict, Rafferty, Howells, & Collins, 1997; Sethuraman & O'Brochta, 2005; White, Coates, Atkinson, & O'Brochta, 1996; Zwiebel et al., 1995), the development and assessment of gene knockdown/silencing methods (Adrianos, Lorenzen, & Oppert, 2018; Colinet et al., 2014; Dong & Friedrich, 2005; Fabrick, Kanost, & Baker, 2004; Khan, Reichelt, & Heckel, 2016; Perera, Little, & Pierce, 2018), and fertility and fecundity studies (Khanh, Bressac, & Chevrier, 2005; Pires, Abrão, Machado, Schofield, & Diotaiuti, 2002), and have been proposed as markers for field and dispersal monitoring (Shimizu & Kawasaki, 2001; Snodgrass, 2002), and as experimental models for aging (Campesan et al., 2011; Navrotskaya & Oxenkrug, 2016; Oxenkrug, 2010; Savvateeva et al., 2000).

The genetic and biochemical architecture of the ommochrome biosynthetic pathway (Figure 1) was initially elucidated using Drosophila mutants exhibiting defects in eye coloring and has since been reconstructed in *Tribolium castaneum* (Grubbs, Haas, Beeman, & Lorenzen, 2015; Lorenzen et al., 2002; Osanai-Futahashi et al., 2015) and *Bombyx mori* (Osanai-Futahashi et al., 2015; Quan et al., 2002; Tatematsu et al., 2011). The primary ommochrome precursor, tryptophan, is imported into eye pigment cells by karmoisin, a monocarboxylate transporter (Dow, 2001; Tearle, 1991), and then enzymatically converted by tryptophan 2,3-dioxygenase (vermilion) to formylkynurenine (Searles & Voelker, 1986; Walker, Howells, & Tearle, 1986). Subsequent processing by a cytosolic enzyme, kynurenine 3-monooxygenase (cinnabar), and a pigment granule localized heme peroxidase (cardinal) yield the precursor ommochrome pigment (Harris, Kim, Nakahara, Vásquez-Doorman, & Carthew, 2011; Warren, Palmer, & Howells, 1996). Heterodimers of ABC transporters (white, scarlet, and brown) embedded in the pigment granule membrane (Mackenzie, Howells, Cox, & Ewart, 2000) facilitate import of the ommochrome (white/scarlet) and pteridine (white/brown) pigment precursors (Dreesen, Johnson, & Henikoff, 1988; Ewart, Cannell, Cox, & Howells, 1994). In *Drosophila*, mutations in the genes *karmoisin*, *vermilion*, *cinnabar*, and/or *cardinal* disrupt the ommochrome biosynthetic pathway, which shifts the balance of pigments to pteridines and results in a red-eye phenotype. Similarly, *scarlet* mutants are characterized by bright red eyes (loss of ommochrome), *brown* mutants by dark brown eyes (loss of pteridine), and *white* mutants by white eyes (complete loss of pigmentation). In contrast, mutations to either *scarlet* or *white* in species that utilize only ommochrome pigments (e.g., *T. castaneum* and *B. mori*) result in white eyes.

Although eye color mutations have been most extensively characterized in dipteran and lepidopteran species, there are descriptions of red-eyed mutants in a number of hemipterans including *Oncopeltus fasciatus* (Dall; Lawrence, 1970), *Geocoris punctipes* (Say; Hagler, 2009), *Laodelphax striatellus* (Fallén; Ishii, 1966; L. H. Wang, Zhuang, Li, & Fang, 2013), *Triatoma infestans* (Insausti, Le gall, & Lazzari, 2013; Moraes et al., 2005; Pires et al., 2002), *Rhodnius prolixus* (Insausti et al., 2013), two species of *Orius* (Shimizu & Kawasaki, 2001), three independent lineages of *Lygus lineolaris* (Allen, 2013; Slaymaker & Tugwell, 1984; Snodgrass, 2002), and multiple *Nilaparvata lugens* (Stål) lines (Jairin, Leelagud, Pongmee, &

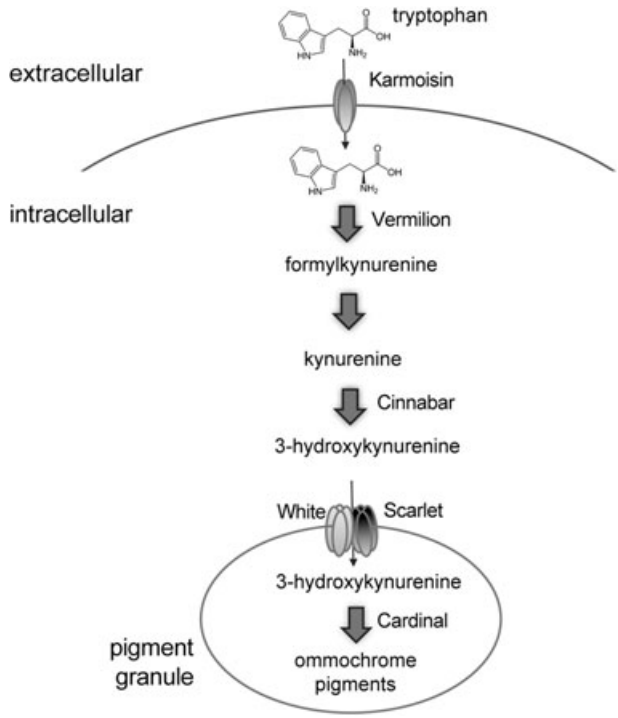

FIGURE 1 Model of ommochrome biosynthesis in insect eye cells. The precursor molecule, tryptophan, is imported into eye pigments cells via a monocarboxylate transporter (karmoisin). The amino acid is then converted to formylkynurenine by tryptophan 2,3-dioxygenase (vermilion). Formylkynurenine is converted either enzymatically or via nonspecific oxidation to kynurenine, which is then hydroxylated to 3-hydroxykynurenine by kynurenine 3-monooxygenase (cinnabar). This compound is actively transported into pigment granules by heterodimers of the ATP-binding cassette transporters white and scarlet (white and brown heterodimers function in pteridine precursor importation). The conversion of 3-hydroxykynurenine to ommochrome pigments requires a heme peroxidase (cardinal). Adapted from Reed and Nagy (2005) and Osanai-Futahashi et al. (2012)

Srivilai, 2017; Liu et al., 2013; Mochida, 1970; Seo, Jung, & Kim, 2011). Despite the prevalence of the red-eye phenotype, molecular characterization of the underlying pigmentation pathways has been largely limited to *N. lugens*. Genetic linkage mapping in this species has placed a red-eye locus between two defined simple sequence repeats on chromosome 9 (Jairin et al., 2017), and RNA interference (RNAi)-mediated knockdown of transcripts homologous to Drosophila *scarlet*, *brown*, *white*, *karmoisin*, *cinnabar*, and *cardinal* confirmed roles in eye pigmentation (Jiang & Lin, 2018; Liu, Luo, Yang, Wang, & Tang, 2017; Liu, Wang, Yang, Luo, & Tang, 2017; Xue et al., 2018). In *L. lineolaris*, the red-eye phenotype in the most recently characterized line was found to be sex-linked (Allen, 2013), rather than under control of an autosomal recessive allele, as reported for the two previous lines (Slaymaker & Tugwell, 1984; Snodgrass, 2002). Although the mutated gene(s) remain to be elucidated, X chromosome-linked eye color mutants in *T. castaneum* have been linked to *cardinal* and *ruby*, the latter of which encodes a protein involved in the biogenesis of lysosome-related organelles, such as pigment granules (Grubbs et al., 2015).

Lygus hesperus Knight is a non-model species sympatric with the closely related *L. lineolaris* that together comprise a complex of morphologically similar polyphagous hemipteran plant bugs in the family Miridae (Schwartz & Foottit, 1998; Wheeler, 2001). In the western United States, *L. hesperus* are significant pests of many economically important crops including cotton, alfalfa, and strawberries (Naranjo, Ellsworth, & Dierig, 2011; Ritter, Lenssen, Blodgett, & Taper, 2010; Scott, 1977; Strand, 2008; Wheeler, 2001). Despite being key pests, molecular resources for *L. hesperus* have only recently been developed (Christie, Hull, Richer, Geib, & Tassone, 2017; Hull, Geib, Fabrick, & Brent,

2013; Hull et al., 2014; Tassone et al., 2016). While injection-based RNAi has been successfully demonstrated for this species (Van Ekert, Wang, Miao, Brent, & Hull, 2016), the ineffectiveness of oral-based RNAi (Allen & Walker, 2012) in *Lygus* limits the overall utility of the method for high throughput functional genomic approaches. Consequently, other techniques, such as the CRISPR/Cas9 system, could prove useful for demonstrating in vivo gene functionality. Although this technique has yet to be applied to *Lygus* bugs, previous studies have demonstrated the utility of targeting eye coloration genes as visible markers for developing CRISPR methods and/or screening phenotypic effects (Adrianos et al., 2018; Khan et al., 2016; F. Li & Scott, 2016; Perera et al., 2018; Xue et al., 2018). However, species-specific functions of eye coloration genes that differ from those described in model systems have been reported (Khan et al., 2016). Consequently, to determine the suitability of various eye coloration genes as CRISPR targets in *L. hesperus*, we sought to initially evaluate phenotypes following RNAi-mediated knockdown. Based on homology with *Drosophila* protein sequences, *L. hesperus* orthologs of *karmoisin*, *vermilion*, *cinnabar*, *cardinal*, *scarlet*, *white*, and *brown* were identified and characterized via phylogenetic inferences, reverse-transcriptase polymerase chain reaction (RT-PCR) profiling, and RNAi-mediated knockdown.

2 | MATERIALS AND METHODS

2.1 | Insect rearing

L. hesperus were obtained from a long-term laboratory colony (USDA-ARS Arid Land Agricultural Research Center, Maricopa, AZ). The stock insects were given unrestricted access to a supply of bean (*Phaseolus vulgaris* L.) pods and an artificial diet mix (Debolt, 1982) packaged in Parafilm M (Pechiney Plastic Packaging, Chicago, IL; Patana, 1982). Both food sources were replenished as needed. Insects were reared at 27.0 ± 1.0°C, 40–60% relative humidity, under a L14:D10 photoperiod. Experimental insects were generated from eggs deposited in Parafilm M agarose packs, with the resulting hatches maintained as above.

2.2 | Bioinformatics

To identify putative *L. hesperus* eye pigmentation genes, previously assembled transcriptomes (Hull et al., 2014; Tassone et al., 2016) were queried using tBLASTn (*e* value ≤ 10^{-5}), with *D. melanogaster* sequences corresponding to the ABC transporters white (AAF45826.1), scarlet (AAF49455.1), and brown (AAA28398.1), as well the ommochrome biosynthetic pathway proteins cardinal (AAF56043.1), cinnabar (AAF59196.4), karmoisin (AAF54851.2), and vermillion (AAF47978.1). The longest variant from the resulting *L. hesperus* sequence hit for each was then re-evaluated against the NCBI nr database with BLASTx (*e* value ≤ 10^{-5}). Conceptually translated sequences were scanned for characteristic protein motifs with ScanProsite (de Castro et al., 2006; Sigrist et al., 2010) and the HMMscan module on the HMMER webserver (Finn, Clements, & Eddy, 2011). Transmembrane (TM) domain predictions were performed using TOPCONS (Bernsel, Viklund, Hennerdal, & Elofsson, 2009). To examine phylogenetic relationships, multiple sequence alignments consisting of the putative *L. hesperus* proteins and sequences (Supporting Information Table S1) from 15 species, representing five insect orders (Coleoptera, Diptera, Hemiptera, Hymenoptera, and Lepidoptera), were constructed using MUSCLE (Edgar, 2004) with default settings implemented in Geneious 10.1.3 (Kearse et al., 2012). Phylogenetic trees were constructed in MEGA X (Kumar, Stecher, Li, Knyaz, & Tamura, 2018). For the figures shown, evolutionary history was inferred by using the maximum likelihood method with the Le–Gascuel model (Le & Gascuel, 2008). The highest log likelihood trees are shown with bootstrap values from 1,000 replicates indicated next to the branches. Trees are drawn to scale, with branch lengths measured in the number of substitutions per site. All positions with <95% site coverage were eliminated, that is fewer than 5% alignment gaps, missing data, and ambiguous bases were allowed at any position (partial deletion option). Initial tree(s) for the heuristic search were obtained automatically by applying Neighbor-Join and BioNJ algorithms to a matrix of pairwise distances estimated using a JTT model, and then selecting the topology with superior log likelihood value. Parameters for specific sequence analyses are as follows: karmoisin—a

discrete γ distribution was used to model evolutionary rate differences among sites (five categories [+G, parameter = 0.9683]) across 16 amino acid sequences with a total of 235 positions in the final data set; vermilion—a discrete γ distribution was used to model evolutionary rate differences among sites (five categories [+G, parameter = 0.4402]) across 16 amino acid sequences with a total of 340 positions in the final data set; cinnabar—a discrete γ distribution was used to model evolutionary rate differences among sites (five categories [+G, parameter = 0.6357]) across 16 amino acid sequences with a total of 290 positions in the final data set; cardinal—a discrete γ distribution was used to model evolutionary rate differences among sites (five categories [+G, parameter = 0.5287]) across 16 amino acid sequences with a total of 386 positions in the final data set; and ABC transporters—a discrete γ distribution was used to model evolutionary rate differences among sites (five categories [+G, parameter = 1.2833]) with rate variation allowing for some sites to be evolutionarily invariable ([+I], 2.26% sites) across 51 amino acid sequences with a total of 531 positions in the final data set. The ABC transporter tree was rooted using the *Leptinotarsa decemlineata* ABC subfamily G member 1-like sequence (XP_023022280.1) as an outgroup.

2.3 | PCR

To confirm the validity of the predicted *L. hesperus* eye pigmentation sequences, full-length open reading frames (ORFs) were PCR amplified and sequenced. Total RNAs were isolated from pooled male and female adult heads (five heads per sex) at 7–9 days posteclosion using TRI Reagent (Life Technologies, Carlsbad, CA) and RNeasy Mini Kit Spin Columns (Qiagen, Germantown, MD). First-strand complementary DNAs (cDNAs) were generated from 500 ng DNase I-treated total RNAs using Superscript III Reverse Transcriptase (Life Technologies) and custom made random pentadecamers (IDT, San Diego, CA). Full-length products were amplified using primers (Supporting Information Table S2) designed to span each of the predicted ORFs. Amplifications were performed using Sapphire Amp Fast PCR Master Mix (Takara Bio USA Inc., Mountain View, CA) in 20-μl volumes, with 0.5 μl cDNA template and 0.15 μM of each primer. Thermocycler conditions consisted of 95°C for 2 min followed by 40 cycles at 95°C for 20 s, 56°C for 20 s, 72°C for 2 min, and a final extension at 72°C for 5 min. The resulting products were separated on 1.5% agarose gels using a Tris/acetate/EDTA buffer system and visualized with SYBR Safe (Life Technologies). Each reaction was subcloned into pCR2.1-TOPO TA (Life Technologies), and sequenced at the Arizona State University DNA Core Laboratory (Tempe, AZ). Consensus sequences have been deposited with GenBank under accession numbers MH806842-MH806848.

For expression profiling analyses, first-strand cDNAs were generated as above and transcript abundance assessed by RT-PCR for two biological replicates of pooled eggs, nymphs (instars 1–5), mixed sex adults (0, 3, 7, 10, and 20 days posteclosion), and the main body segments (head, thorax, and abdomen) of Days 7–9 mixed sex adults. Fragments (~ 500 bp) of the *L. hesperus* transcripts were amplified from each biological replicate as above using gene-specific primers (Supporting Information Table S2). A ~500-bp fragment of *L. hesperus* actin (GBHO01044314.1) was likewise amplified, as a positive indicator of cDNA quality. Thermocycler conditions consisted of 95°C for 2 min followed by 35 cycles at 95°C for 20 s, 56°C for 20 s, and 72°C for 30 s, and a final extension at 72°C for 5 min. PCR products were separated on 1.5% agarose gels and visualized as before. Gel images were obtained using an AlphaImager Gel Documentation System (ProteinSimple, San Jose, CA), then processed in Photoshop CS6 v13.0 (Adobe Systems Inc., San Jose, CA).

2.4 | RNAi-mediated knockdown

The complete 687-bp ORF of venus (a yellow fluorescent protein variant) and ~500 bp fragments of the seven *L. hesperus* eye color-associated sequences were amplified from validated plasmid DNAs using primers (Supporting Information Table S2) containing a 5′ T7 promoter sequence (TAATACGACTCACTATAGGGAGA) and Sapphire Amp Fast PCR Master Mix. Thermocycler conditions consisted of 95°C for 2 min followed by 35 cycles at 95°C for 20 s, 61°C for 20 s, and 72°C for 30 s, and a final extension at 72°C for 5 min. The resulting PCR products were gel

purified with an EZNA Gel Extraction Kit (Omega Bio-Tek, Norcross, GA), then used with a MEGAscript RNAi Kit (Life Technologies) to generate double-stranded RNAs (dsRNAs) according to the manufacturer's instructions. Purified dsRNAs were quantitated on a Synergy H4 Hybrid Multi-Mode Microplate Reader (BioTek Instruments, Winooski, VT), then diluted to 1 μg/μl in MEGAscript RNAi Kit elution buffer. Following cold immobilization on ice for 5 min, 1-day-old fifth instars were injected between the fifth and seventh abdominal tergites with 250 μl of the 1-μg/μl dsRNAs using a Nanoject III Programmable Nanoliter Injector (Drummond Scientific Company, Broomall, PA) fitted with a 5-μl disposable soda lime glass pipet needle (Thermo Fisher Scientific, Kimble Chase, Pittsburgh, PA). Injection needles were made using a magnetic glass microelectrode horizontal puller (PN-30; Narishige, Tokyo, Japan) set at heater level 84.4 and magnet level 25.5. Injected nymphs were allowed to recover for 10 min, then maintained under normal rearing conditions. Those that failed to recover were discarded. Treatment groups consisted of 40 nymphs of each sex per dsRNA set, with three replicates of each. Groups were housed in individual 1,890 ml waxed chipboard cups (Huhtamaki, De Soto, KS) covered with nylon mesh to ensure adequate ventilation and light exposure. Cups were provisioned with approximately 20 g of fresh green bean pods and 1 g of raw sunflower (*Helianthus annuus* L.) seeds, which were replaced every 48 hr. Rearing cups were placed in incubation chambers under the same conditions specified for the stock colony. Groups were inspected daily for mortality, then frozen at 7 days postinjection. To determine the strength and consistency of these knockdowns, all surviving females and males had their resultant phenotypes scored based on the degree to which the pattern of eye coloration deviated from that observed in untreated individuals of the same gender reared under the same conditions. A "zero" was scored when there was no deviation from this norm, a "one" when there were visible but subtle changes, and a "two" for clearly discernable differences.

Subsets of each replicated group were assayed by RT-PCR to confirm target transcript knockdown using the 500-bp primers described above and thermocycler conditions consisting of 95°C for 2 min followed by 35 cycles at 95°C for 20 s, 56°C for 20 s, and 72°C for 30 s, and a final extension at 72°C for 5 min. PCR products were electrophoresed and visualized as before with gel images processed (auto tone and enhanced contrast) in Photoshop CS6 v13.0. Band intensities of electrophoresed PCR products were calculated in Fiji (Schindelin et al., 2012) implementation of Image J. Values were normalized to actin levels and then calculated relative to those of products amplified from individuals injected with *venus* dsRNAs. Statistical comparisons were made using GraphPad Prism v. 6.0 for Mac OS X (GraphPad Software, La Jolla, CA) using a one-way analysis of variance (ANOVA) across treatments followed by multiple paired comparisons between treatments and their respective controls using the Holm–Sidak method.

3 | RESULTS

3.1 | Identification and bioinformatic analyses

To identify putative *L. hesperus* homologs of Drosophila *karmoisin*, *vermilion*, *cinnabar*, *cardinal*, *white*, *scarlet*, and *brown*, we used a tBLASTn search to scan available *L. hesperus* transcriptomic data (Hull et al., 2014; Tassone et al., 2016). Sequences encompassing complete ORFs with 30–67% sequence identity to the seven query proteins were identified (Table 1); for simplicity, they will be referred to as *LhKar* (*karmoisin*), *LhV* (*vermilion*), *LhCn* (*cinnabar*), *LhCd* (*cardinal*), *LhW* (*white*), *LhSt* (*scarlet*), and *LhBw* (*brown*). BLASTx analysis of the predicted ORFs revealed top hits consistent with the initial annotations (Supporting Information Table S3). The *LhW*, *LhSt*, and *LhBw* transcripts correspond to three previously identified ABCG transporter subfamily members: LhABCG10, LhABCG12, and LhABCG7, respectively (Hull et al., 2014). In that study of *L. hesperus* ABC transporters, two additional partial sequences (LhABCG8 and LhABCG9) were found to phylogenetically cluster with other brown-like sequences; however, because those sequences lacked start codons, we have limited our analyses in the current study to the complete ORF encompassing the *LhBw* transcript.

To confirm the validity of the transcriptomic data, the respective ORFs for the predicted *L. hesperus* eye coloration genes were amplified from adult head cDNAs. In all cases, nucleotide sequence identity of the predicted

TABLE 1 Transcriptome-based identification of eye pigmentation gene homologs in *Lygus hesperus*

Targets	Local transcript	BioProject PRJNA284294	BioProject PRJNA238835	GenBank	Seq Id (%)[a]	ORF (bp)	No. of amino acids
karmoisin (*LhKar*)	c86058_g4_i1	GDHC01010560.1	GBHO01031048.1	MH806845	44.3	1,296	431
vermilion (*LhV*)	c65070_g1_i1	GDHC01009857.1	GBHO01020750.1	MH806846	67.5	1,185	394
cinnabar (*LhCn*)	c84242_g1_i1	n/a	GBHO01042047.1	MH806847	51.5	1,359	452
cardinal (*LhCd*)	c87023_g1_i2	GDHC01003684.1	GBHO01041848.1	MH806848	39.8	2,250	749
white (*LhW*)	c90268_g1_i1	GDHC01004115.1	GBHO01021188.1	MH806842	50.3	2,115	704
scarlet (*LhSt*)	c83759_g1_i1	GDHC01001306.1	GBHO01041190.1	MH806843	43.0	1,704	567
brown (*LhBw*)	c83541_g1_i5	GDHC01016572.1	GBHO01020554.1	MH806844	30.1	1,827	608

[a]Percent sequence identity with Drosophila protein.

ORFs between the consensus sequences and the transcriptomic data exceeded 99%. The consensus cloned *LhSt* sequence (derived from multiple independent PCR amplifications), however, differed from the transcriptomic sequence via a stop codon in a homopolymeric region at nucleotide 28 that translocated the first in-frame ATG start 261 bases downstream of the predicted location. As a result, the complete verified ORF is 1,704 nt in length rather than 1,965 nt. The consensus cloned sequences have been submitted to GenBank under the following accession numbers: *LhW* (MH806842), *LhSt* (MH806843), *LhBw* (MH806844), *LhKar* (MH806845), *LhV* (MH806846), *LhCn* (MH806847), and *LhCd* (MH806848).

Structural domain analyses of the *L. hesperus* proteins revealed features consistent with the initial annotations (Supporting Information Table S4). As a predicted monocarboxylate transporter (Halestrap, 2012), LhKar has 12 TM domains, dual intracellular termini, and a relatively large intracellular loop between TMs 6–7. LhCn and LhCd are likewise predicted to be membrane-bound proteins. LhCn has the FAD-binding domain (Pfam PF01494) typical of flavin-dependent hydroxylases, such as kynurenine 3-monooxygenase (Han, Beerntsen, & Li, 2007), whereas LhCd has the heme-dependent peroxidase domain (Pfam PF03098) necessary for ommochrome synthesis (Harris et al., 2011; Osanai-Futahashi et al., 2015). LhCd, however, exhibits atypical secondary structure with two predicted TM segments rather than the single C-terminal TM domain common to most Cd homologs. In addition, a highly conserved tryptophan, presumed critical for peroxidase activity (Osanai-Futahashi et al., 2015), has been replaced with methionine in LhCd and a number of other hemipteran sequences (Supporting Information Figure S1). The absence of defined helical segments in the LhV sequence, combined with the presence of a tryptophan dioxygenase signature (Pfam PF03301), is consistent with a role as the initial enzyme in ommochrome biosynthesis (i.e., tryptophan 2,3-dioxygenase). The single ATP-binding domain and six TM segments predicted in LhW, LhSt, and LhBw support their classification as half transporters and suggest that their functionality is dependent on dimerization (Wilkens, 2015). ABC transporters associated with the importation of pigment precursors can be differentiated from non-pigment transporters by a (C/L)DEPT motif in the Walker B functional domain and by an IHQP motif in the H-loop domain that functions in ATP hydrolysis (Grubbs et al., 2015). This latter motif is present in the three putative Lh transporters (Supporting Information Figure S2), whereas the (C/L)DEPT motif is only present in LhW and LhBw. LhSt has a conservative Val substitution of the C/L position. In addition, LhBw has the 6–9 amino acid deletion upstream of the (C/L)DEPT motif that is characteristic of Brown orthologs (Grubbs et al., 2015).

3.2 | Phylogenetic analyses

Maximum likelihood trees were constructed to examine the phylogenetic relationships of the respective *L. hesperus* sequences with homologous proteins from representative species across five insect orders (Diptera, Coleoptera, Hymenoptera, Hemiptera, and Lepidoptera). LhKar and LhCd sorted with sequences from other hemipterans in

order-specific clades (Figure 2a,d). The other two ommochrome pathway proteins did not exhibit order-specific clustering (Figure 2b,c). Although pairwise sequence identity of LhCn with sequences from the other four orders ranged from 45.5% to 52.8%, it and a predicted kynurenine 3-monooxygenase from *Acyrthosiphon pisum* (hemiptera) clustered with coleopteran sequences in a clade separate from the other putative cinnabar proteins (Figure 2c). In contrast, none of the hemipteran vermilion sequences, including LhV, aligned to a clade (Figure 2b). Rather, the phylogenetic sorting of the four sequences, particularly the *A. pisum* protein, was comparable with that of an outgroup. Although this could be an indication of significant order-specific divergence, *LhV* shares 67% pairwise sequence identity with the *Drosophila* sequence, and has structural features (Supporting Information Table S4) consistent with its annotation. The unexpected phylogenetic clustering of *LhV* and *LhCn* does not appear to be misannotation, as each sequence was unique in the *L. hesperus* transcriptomic data sets with no other homologous transcripts exhibiting comparable sequence identities. Consequently, the observed clustering, which was observed in other phylogenetic inferences, may be an artifact of the limited number of order-specific sequences incorporated. Regardless of, clustering of the four *L. hesperus* sequences with homologous sequences supports their annotation as ommochrome pathway genes.

Phylogenetic relationships of the three *L. hesperus* ABC transporter sequences (LhW, LhSt, and LhBw) were consistent with a previous report (Hull et al., 2014) and were largely order-specific (Figure 3). LhBw, however, clustered in a subfamily-specific clade consisting of Brown paralogs termed "Ok," which were initially identified in *B. mori* and have since been shown in lepidopterans to function in the transport of uric acid rather than pteridines (Khan et al., 2016; L. Wang, Kiuchi, et al., 2013). Brown-like sequences (i.e., Brown and Ok) are the least conserved of the eye pigment transporters (Supporting Information Table S5) and are thought to have arisen from duplication of an ancestral *brown* (L. Wang, Kiuchi, et al., 2013), an event that is supported by our phylogenetic analysis. Although annotated as "Brown," LhBw did not sort with the Brown subfamily, nor did any of the other hemipteran sequences, including those annotated in previous studies as Brown orthologs (e.g., *N. lugens brown*). Our analyses, coupled with a previous study that found multiple *ok* orthologs in the pea aphid *A. pisum* but no *brown* orthologs (L. Wang, Kiuchi, et al., 2013), suggests an evolutionary loss of the duplicated *brown* in the hemipteran lineage.

3.3 | RT-PCR expression profiling

To elucidate functional roles, we examined the expression of the respective eye color-associated transcripts in eggs, across nymphal development, and in adults at varying points of maturation. Transcripts for the three ABC transporters (*LhW*, *LhSt*, and *LhBw*) were amplified to varying degrees from all stages of development with little or no difference observed in expression between the nymphal stages, immature adults, and mature adults (Figure 4a). Similar expression profiles were seen for both *LhKar* and *LhV*. Although no PCR amplimers were generated from egg cDNAs for *LhCn* and *LhCd*, they were present from the first nymphal stage onward. We also examined expression in the body segments of reproductively mature adults (i.e., 7 days posteclosion). As before, ABC transporter expression was ubiquitous (Figure 4b). *LhCn* expression was head-specific, whereas *LhKar*, *LhV*, and *LhCd* exhibited a more varied expression profile but with transcripts predominantly in the head.

3.4 | RNAi-mediated knockdown

In our *L. hesperus* colony, adult female eyes are uniformly dark brown from eclosion through reproductive maturation (i.e., 7 days posteclosion), whereas newly emerged male eyes are brown with a reddish band along the medial margin that darkens to a uniform brown over time (Figure 5a). A red-eye mutant, which occurs at extremely low frequencies in our *L. hesperus* colony, had orange-red eyes (Figure 5b) similar to that described previously in *L. lineolaris* (Allen, 2013; Slaymaker & Tugwell, 1984; Snodgrass, 2002).

To examine the functional role of the putative ommochrome biosynthetic pathway genes on *L. hesperus* eye coloration, we injected dsRNAs corresponding to ~500 bp fragments of the respective coding sequences. Control

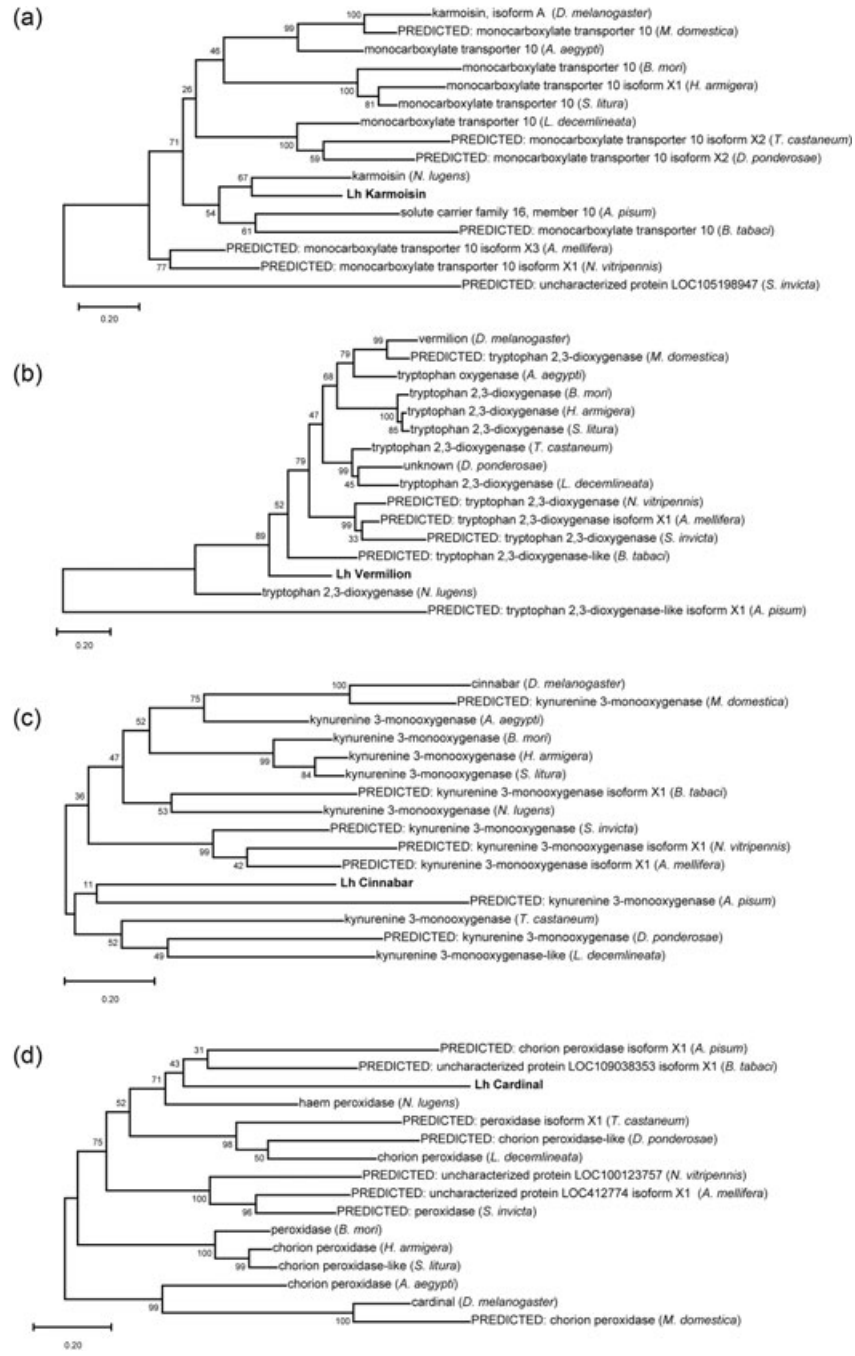

FIGURE 2 Maximum likelihood trees depicting the phylogenetic relationship between *Lygus hesperus* ommochrome biosynthesis-related transcripts and homologs from five insect orders: (a) karmoisin, (b) vermilion, (c) cinnabar, and (d) cardinal. Bootstrap support values are indicated at the nodes. The *L. hesperus* sequences are shown in bold font. Sequence descriptors correspond to NCBI annotations. Species abbreviations—*A. pisum*: *Acyrthosiphon pisum*; *B. tabaci*: *Bemisia tabaci*; *B. mori*: *Bombyx mori*; *D. ponderosae*: *Dendroctonus ponderosae*; *D. melanogaster*: *Drosophila melanogaster*; *H. armigera*: *Helicoverpa armigera*; *L. decemlineata*: *Leptinotarsa decemlineata*; *M. domestica*: *Musca domestica*; *N. lugens*: *Nilaparvata lugens*; *S. invicta*: *Solenopsis invicta*; *S. litura*: *Spodoptera litura*; *T. castaneum*: *Tribolium castaneum*; *N. vitripennis*: *Nasonia vitripennis*. Similar topologies were generated with other phylogenetic algorithms. Accession numbers for sequences used in the analyses are listed in Supporting Information Table S1

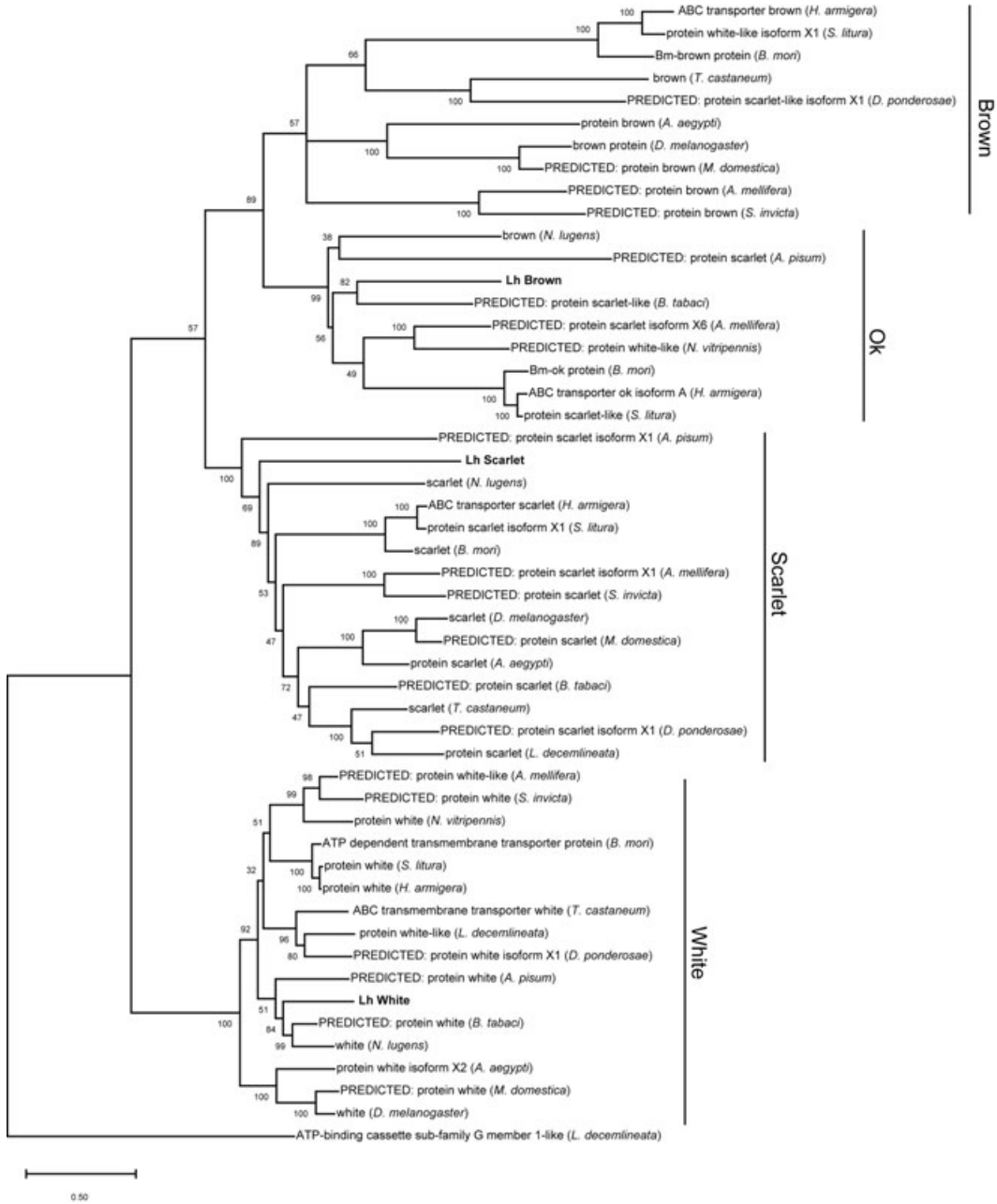

FIGURE 3 Maximum likelihood tree depicting the phylogenetic relationship between *Lygus hesperus* pigment-associated ATP-binding cassette (ABC) transporters and homologs from five insect orders. Bootstrap support values are indicated at the nodes. The *L. hesperus* sequences are shown in bold font. Sequence descriptors correspond to NCBI annotations. Species abbreviations are as in Figure 2. The tree was rooted using the *Leptinotarsa decemlineata* ATP-binding cassette subfamily G member 1-like sequence (XP_023022280.1). Similar topologies were generated with other phylogenetic algorithms. Accession numbers for sequences used in the analyses are listed in Supporting Information Table S1

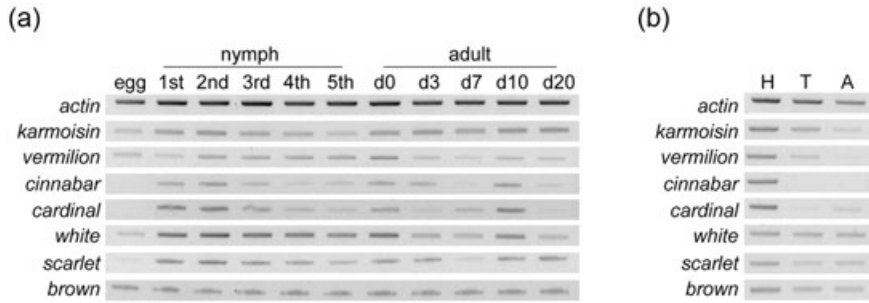

FIGURE 4 Expression profile of *Lygus hesperus* eye color-associated transcripts. (a) Developmental expression of transcripts from egg through nymphal development (1st–5th), and at varying points in adult maturation including adults at 0 days (d0), 3 days (d3), 7 days (d7), 10 days (d10), and 20 days (d20) posteclosion. (b) Expression in 7-day-old body segments (H: head; T: thorax; A: abdomen). Amplimers correspond to ~500 bp fragments of the transcripts of interest. For better band clarity, the negative images of representative gels corresponding to two biological replicates of pooled complementary DNAs are shown

females and males were injected with dsRNA corresponding to the *Venus* ORF. None of the knockdowns resulted in the bright red-orange phenotype characteristic of the *L. hesperus* mutant. Individuals injected with dsRNAs for *LhKar*, *LhV*, *LhCn*, *LhCd*, and *LhSt* exhibited a clear bifurcation of eye coloration similar to that seen in newly enclosed males, with a sharp red to red-orange band along the medial margin extending from the rostral terminus to the antenna (Figure 5c). In contrast, knockdown of *LhW* and *LhBw* resulted in adult eyes uniformly colored pale brown (Figure 5c). No changes to eye color were seen in adults injected with *venus* dsRNA. When scored for phenotype strength, *LhCd* produced the strongest and most consistent knockdown effect of any of the treatments (Table 2), although the other dsRNAs also had discernable effects in most individuals. Taken together, these results support a role for ommochrome biosynthesis in *L. hesperus* eye coloration and suggest that, unlike *Tribolium* and *Bombyx* (Grubbs et al., 2015; Lorenzen et al., 2002; Quan et al., 2002; Tatematsu et al., 2011), both ommochromes and pteridine pigments contribute to coloration.

LhW knockdown produced other effects beyond eye coloration, causing adults to be smaller with soft, sticky cuticles that were paler in color than controls (Figure 5d). Behaviorally, individuals injected with *LhW* dsRNAs were lethargic and unresponsive to normal disturbance cues. Despite exhibiting an eye coloration phenotype similar to that of the *LhW* knockdown, adults injected with dsRNAs corresponding to *LhBw* did not exhibit the cuticular or behavioral defects (Figure 5d). Consistent with the observed phenotypes, RT-PCR confirmed injected dsRNAs significantly impacted transcript levels in adults at 7 days postinjection (Figure 6; ANOVA, $F = 7.381$, $df = 13$, $P < 0.001$). Specifically, reductions relative to controls were confirmed for *LhKar* (Holm–Sidak; $t = 4.389$, $P < 0.001$), *LhV* ($t = 3.412$, $P = 0.002$), *LhCn* ($t = 2.684$, $P = 0.012$), *LhCd* ($t = 3.030$, $P = 0.005$), *LhW* ($t = 3.239$, $P = 0.003$), *LhSt* ($t = 4.083$, $P < 0.001$), and *LhBw* ($t = 2.378$, $P = 0.024$).

4 | DISCUSSION

Although numerous genes involved in eye coloration have been identified and successfully utilized as transgenic markers in a number of insect species (Coates, Jasinskiene, Miyashiro, & James, 1998; Cornel et al., 1997; Fridell & Searles, 1991; White et al., 1996; Zwiebel et al., 1995), the associated eye color phenotypes are not always conserved across species. In *D. melanogaster* and *S. americana*, disruption of *vermilion* results in a red-eye phenotype (Dong & Friedrich, 2005; Walker et al., 1986), whereas in *Helicoverpa armigera*, *Musca domestica*, and *T. castaneum* mutations of the same gene yielded yellow, green, and white eyes (Lorenzen et al., 2002; Perera et al., 2018; White

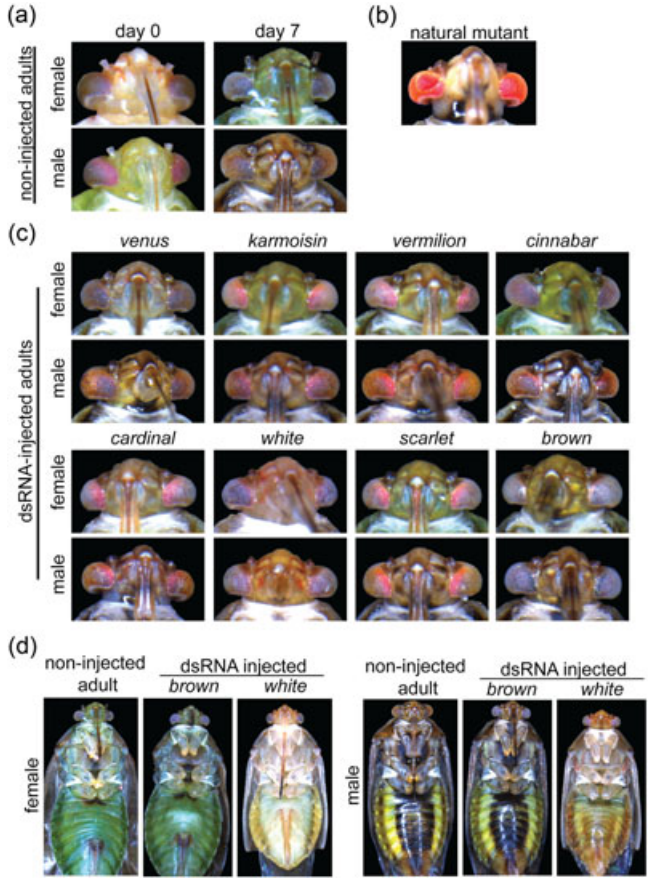

FIGURE 5 Effects of RNA interference-mediated knockdown on *Lygus hesperus* eye coloration. (a) Wildtype male and female *L. hesperus* on the day of eclosion and as 7-day-old adults. (b) Red-eyed *L. hesperus* mutant. (c) Eye coloration in adult male and female *L. hesperus* 7 days after injection with double-stranded RNAs (dsRNAs) targeting the indicated eye pigment-associated gene. Eye color in individuals injected with *venus* dsRNA was indistinguishable from wildtype, whereas knockdown of each of the targeted genes altered the pigmentation pattern in both adult male and female *L. hesperus*. Images are representative of three biological replicates consisting of 40 bugs from each sex. (d) Full-body images of noninjected *L. hesperus* adults and those injected as fifth instars with dsRNAs corresponding to *brown* and *white*. Individuals injected with *white* dsRNAs consistently exhibited smaller bodies with softer, sticky cuticles that were paler in color than controls. Images are representative of three biological replicates consisting of 40 bugs of each sex

et al., 1996). Similarly, *cinnabar* mutations manifest as red eyes in *D. melanogaster*, *Leptopilina boulardi*, *Nasonia vitripennis*, and *N. lugens* (Colinet et al., 2014; M. Li et al., 2017; Warren et al., 1996; Xue et al., 2018), but are white in *T. castaneum*, *B. mori*, and *Aedes aegypti* (Aryan, Anderson, Myles, & Adelman, 2013; Lorenzen et al., 2002; Quan et al., 2002). While these differences likely reflect variations in the quantity and chemical nature of compounds (e.g., ommochrome and pteridine) that accumulate in the eye pigment granules, functional divergence of the underlying genes can also lead to phenotypic variation (Grubbs et al., 2015; Khan et al., 2016). As a result of this interspecific variability, we used an RNAi approach to assess the suitability of eye coloration genes as potential markers for the non-model hemipteran pest, *L. hesperus*.

The majority of genes tested produced a similar novel phenotype with a distinctive red band running along the margin of the eye (Figure 5c), making them viable candidates. In contrast, *LhW* knockdown produced a variety of

TABLE 2 *Lygus hesperus* eye coloration characteristics and statistics of RNAi knockdown

Treatments	*n*	Mean[a]	*SD*	Eye color description
Noninjected	30	0.37	0.56	Uniform dark brown
venus dsRNA	30	0.23	0.43	Uniform dark brown
karmoisin dsRNA	30	1.33	0.61	Red band along the medial margin extending from the rostral terminus to the antenna, remainder light brown
vermilion dsRNA	30	1.33	0.61	Red band along the medial margin extending from the rostral terminus to the antenna, remainder light brown
cinnabar dsRNA	30	1.2	0.76	Narrow red band along the medial margin extending from the rostral terminus to the antenna, remainder dark brown
cardinal dsRNA	30	1.6	0.5	Red band along the medial margin extending from the rostral terminus to the antenna, remainder light brown
white dsRNA	28	1.29	0.76	Uniform light brown
scarlet dsRNA	30	1.3	0.79	Red band along the medial margin extending from the rostral terminus to the antenna, remainder light brown
brown dsRNA	30	1.23	0.86	Uniform light brown

Note. dsRNA: double-stranded RNA; RNAi: RNA interference.

[a]Mean calculated from individual pigmentation scores: 0 = *no difference from control*, 1 = *small difference*, 2 = *clear difference.*

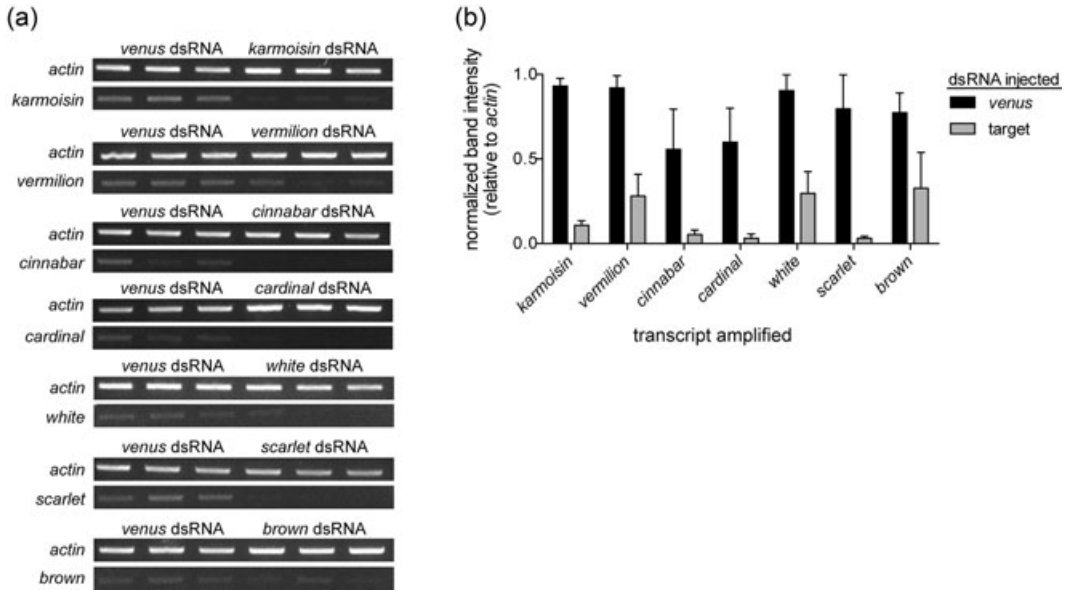

FIGURE 6 Effects of RNA interference-mediated knockdown on transcript levels. (a) Reverse-transcriptase polymerase chain reaction (RT-PCR) was performed using complementary DNAs generated 7 days after double-stranded RNAs (dsRNA) injection. Amplimers correspond to ~500 bp fragments of the indicated genes. Gels shown are representative images. Note that each group of PCR products were electrophoresed on the same gel and imaged under the same conditions. (b) Mean (± *SEM*) values for semiquantitative band analysis of PCR products shown in the gel images. Values were normalized to actin levels and are relative to expression in individuals injected with *venus* dsRNAs. All comparisons between target genes and their controls differed significantly (Holm–Sidak; $P < 0.05$)

undesirable physiological and behavioral effects in *L. hesperus*. This differs from a number of species in which disruption of *white* results in apparently normal adults with nonpigmented white eyes (Benedict, Besansky, Chang, Mukabayire, & Collins, 1996; Grubbs et al., 2015; Jiang & Lin, 2018; Loukeris, Livadaras, Arc, Zabalou, & Savakis, 1995; Mackenzie et al., 1999; Tsuji et al., 2018; Xue et al., 2018). Phenotypic changes modulated by *white* beyond eye coloration, however, have been reported for Drosophila with effects on courtship behavior (Anaka et al., 2008; Krstic, Boll, & Noll, 2013), biogenic amine distribution (Borycz, Borycz, Kubow, Lloyd, & Meinertzhagen, 2008), sensitivity to anesthetics (Campbell & Nash, 2001), stress tolerance (Ferreiro et al., 2018), and recovery from anoxia (Xiao & Robertson, 2016). Outside of Drosophila, elevated *white* transcript levels following xenobiotic exposure in *Mayetiola destructor* and *N. lugens* have been posited as evidence for a role in detoxification (Liu, Yang, Wang, Luo, & Tang, 2018; Shukle, Yoshiyama, Morton, Johnson, & Schemerhorn, 2008). In Lepidoptera, *white* mutations have been associated with multiple phenotypes, including embryonic lethality in *H. armigera* (Khan et al., 2016), and impaired uric acid deposition in *B. mori* and *H. armigera* that results in larvae with a translucent epidermis (Khan et al., 2016; Kômoto, Quan, Sezutsu, & Tamura, 2009). While the *LhW* knockdowns produced a reduction in pigmentation, the role of uric acid in cuticular coloring is unknown for *Lygus* species, so a different mechanism may be in operation. The persistent sticky cuticle of adults injected with *LhW* dsRNAs could indicate a functional role of LhW in molting, in particular, reuptake of the molt fluid. A similar "wet" cuticle phenotype and molting-related defects were reported in *H. armigera* larvae with CRISPR-induced mutations in *white* (Khan et al., 2016). Given the potential fitness costs associated with the pleiotropic functionalities of LhW and its broad expression profile, which could indicate roles in embryonic development, *LhW* would be a poor candidate marker for CRISPR-based disruption.

Eye coloration produced by knockdown of *LhBw* was similar to that of *LhW*, but without the additional physiological and behavioral effects. In drosophilids, the importation of red-colored pteridine precursors is facilitated by heterodimerization of Brown and White such that disruption of Brown functionality shifts the balance of pigments towards ommochromes that cause eyes to appear brown (Dreesen et al., 1988; Mackenzie, Howells, Cox, & Ewart, 2012). Similar functionality has been reported in *N. lugens*; RNAi-mediated knockdown of *brown* transcripts affected eye coloration and reduced pteridine levels in early instar nymphs (Jiang & Lin, 2018). The effects on adult eye pigmentation (i.e., reduced color intensity) observed following injection of *LhBw* dsRNAs (Figure 5C) suggests that *L. hesperus* eye coloration is derived from both ommochrome and pteridine-based pigments and that the role of Brown in pteridine transport has been conserved in hemipterans. Brown functionality and pteridine pigment utilization, however, are not universal across the Insecta. Disruption of Brown function in *B. mori* and *H. armigera* had no visible effects on eye coloration or larval cuticle pigmentation (Khan et al., 2016; Zhang, Kiuchi, Hirayama, Katsuma, & Shimada, 2018). Similarly, RNAi-mediated knockdown of *brown* transcripts in *T. castaneum* had no visible phenotypic effects (Grubbs et al., 2015). The authors of that study suggested that the reduced role of pteridines in some species lessened evolutionary constraints on *brown*, which resulted in varied substrate utilization and greater sequence divergence. In support of this, Brown functionality has been linked to anesthetic sensitivity and biogenic amine transport in Drosophila (Borycz et al., 2008; Campbell & Nash, 2001), and uptake of riboflavin by *B. mori* Malpighian tubules (Zhang et al., 2018). Furthermore, *brown* is the least conserved of the pigment transporter genes (see Supporting Information Table S5 and Grubbs et al., 2015), a fact that likely contributed to early reports suggesting that it had been lost in a number of insect lineages (Broehan, Kroeger, Lorenzen, & Merzendorfer, 2013; Tatematsu et al., 2011). Multiple *brown*-like sequences, however, have since been identified in the transcriptomic/genomic data of diverse species (Grubbs et al., 2015; Khan et al., 2016; L. Wang, Kiuchi, et al., 2013; Zhang et al., 2018). In *B. mori*, the Brown paralog Ok dimerizes with White to facilitate transport of uric acid into epidermal pigment granules, but, similar to Brown, does not function in the import of eye pigments (L. Wang, Kiuchi, et al., 2013). The *H. armigera* Ok likewise functions in uric acid transport and has no role in eye coloration (Khan et al., 2016). We previously identified two additional ABCG sequences (LhABCG8 and LhABCG9) in *L. hesperus* that clustered phylogenetically with Brown-like sequences (Hull et al., 2014). Given the divergent phenotype produced by knocking down of *LhW* (reduced eye and cuticle coloration) and *LhBw* (reduced eye

coloration), we speculate that the cuticular phenotype arises from LhW heterodimerization with one of the other ABCG sequences, and that the eye phenotype results from pteridine import facilitated by the LhW-LhBw dimer. Consequently, even though phylogenetic analyses suggest LhBw is most similar to Ok paralogs, it is functionally more analogous to the *D. melanogaster* Brown, thus we suggest that our initial brown annotation is most relevant.

Although targeted knockdown of genes in the *L. hesperus* ommochrome pathway (*LhV*, *LhCn*, and *LhCd*) and pigment transporters (*LhKar*, *LhW*, *LhSt*, and *LhBw*) had clear effects on adult eye coloration (Figure 5c), the phenotypes do not replicate the characteristic uniform coloring of a *L. hesperus* red-eyed mutant (Figure 5b; Allen, 2013). Similar incomplete mosaic phenotypes were reported following RNAi knockdown of the three pigment-associated ABC transporters as well as *karmoisin* and *cinnabar* in *N. lugens* (Jiang & Lin, 2018; Liu, Luo, et al., 2017; Liu, Wang, et al., 2017; Xue et al., 2018). This limited knockdown might be attributable to poor penetrance of the dsRNAs into pigment containing cells of the eye and/or reflect the limited transcript reduction capability of RNAi. Changes induced by alternative approaches, such as CRISPR, might produce a superior phenotype by achieving a total knockout of the targeted genes. Alternatively, a number of studies have reported homogenous alterations in eye coloration following knockdown of various genes associated with eye pigmentation (Colinet et al., 2014; Grubbs et al., 2015; Liu, Luo, et al., 2017; Tsuji et al., 2018), suggesting that the observed *L. hesperus* phenotypes may reflect the influence of a developmental trait rather than a methodological effect. Retinal cells in *S. americana* undergo progressive development with each nymphal stage and show little to no turnover of pigmentation after differentiation (Dong & Friedrich, 2005). Consequently, disruption of ommochrome biosynthesis and/or import would have no effect on pigment accumulation in cells that had already undergone differentiation and could thus generate a phenotype similar to that seen in our knockdowns. This is supported by the observation that eye coloration in newly emerged adult *L. hesperus* males (and to lesser extent females) is not uniform, with a lighter hued band extending from the rostral terminus to the antenna that darkens over time (Figure 5a). This band aligns with the red region seen in the knockdowns (Figure 5c). The development of deeper hued coloration in this region likely corresponds to cells undergoing active ommochrome/pteridine biosynthesis and import. Consequently, manipulating points along that pathway via RNAi would disrupt the nature and quantity of pigments generated and thus affect eye coloration similar to that seen in our knockdowns. Further, disrupting gene function earlier in development, such as would occur with the natural mutant, should then produce a more uniform eye color in adults.

In summary, using available transcriptomic resources for *L. hesperus* we identified putative homologs of genes shown in other species to function in eye pigmentation. Consistent with their proposed role, each of the genes was expressed in adult heads as well as throughout nymphal and adult development. Their roles in eye coloration were confirmed via RNAi-mediated knockdown with the most pronounced pigmentation effects observed following knockdown of *LhCd*, *LhKar*, and *LhV* transcripts (Table 2). Given that the purpose of this study was to determine the suitability of eye coloration genes as targets for developing gene editing methods in *Lygus* species, we have concluded that *LhCd* will likely prove to be the most effective marker. Its disruption generated a robust visible phenotype applicable to high throughput screening. Furthermore, the lack of *LhCd* transcripts in eggs coupled with predominant head expression suggests limited embryonic/developmental function. Despite its utility in other species, the aberrant cuticular and behavior effects generated following *LhW* knockdown indicate that it would be the least suitable of the genes screened.

ACKNOWLEDGMENTS

The authors thank Mr. Daniel Langhorst for assistance with dsRNA injections, Ms. Missy Tran for her efforts with the pilot study, Ms. Lauren Fabrick for assistance scoring phenotypic effects, and Dr. Jeffrey A. Fabrick for providing the *Lygus hesperus vermilion* T7 primers. Funding was provided by Cotton Inc. (16–410) to C. S. B. and J. J. H. Mention of trade names or commercial products in this study is solely for the purpose of providing specific information and does not imply recommendation or endorsement by the US Department of Agriculture (USDA). USDA is an equal opportunity provider and employer.

ORCID

Colin S. Brent http://orcid.org/0000-0003-2078-1417

REFERENCES

Adrianos, S., Lorenzen, M., & Oppert, B. (2018). Metabolic pathway interruption: CRISPR/Cas9-mediated knockout of tryptophan 2,3-dioxygenase in *Tribolium castaneum*. *Journal of Insect Physiology*, *107*, 104–109.

Allen, M. L. (2013). Genetics of a sex-linked recessive red eye color mutant of the tarnished plant bug, *Lygus lineolaris*. *Open Journal of Animal Sciences*, *03*, 1–9.

Allen, M. L., & Walker, W. B. (2012). Saliva of *Lygus lineolaris* digests double stranded ribonucleic acids. *Journal of Insect Physiology*, *58*, 391–396.

Anaka, M., MacDonald, C. D., Barkova, E., Simon, K., Rostom, R., Godoy, R. A., … Lloyd, V. (2008). The white gene of *Drosophila melanogaster* encodes a protein with a role in courtship behavior. *Journal of Neurogenetics*, *22*, 243–276.

Aryan, A., Anderson, M. A. E., Myles, K. M., & Adelman, Z. N. (2013). TALEN-based gene disruption in the dengue vector *Aedes aegypti*. *PLOS One*, *8*, e60082.

Beard, C. B., Benedict, M. Q., Primus, J. P., Finnerty, V., & Collins, F. H. (1995). Eye pigments in wild-type and eye-color mutant strains of the African malaria vector *Anopheles gambiae*. *The Journal of Heredity*, *86*, 375–380.

Benedict, M. Q., Besansky, N. J., Chang, H., Mukabayire, O., & Collins, F. H. (1996). Mutations in the *Anopheles gambiae* pink-eye and white genes define distinct, tightly linked eye-color loci. *The Journal of Heredity*, *87*, 48–53.

Bernsel, A., Viklund, H., Hennerdal, A., & Elofsson, A. (2009). TOPCONS: Consensus prediction of membrane protein topology. *Nucleic Acids Research*, *37*, W465–W468.

Borycz, J., Borycz, J. A., Kubow, A., Lloyd, V., & Meinertzhagen, I. A. (2008). Drosophila ABC transporter mutants white, brown and scarlet have altered contents and distribution of biogenic amines in the brain. *Journal of Experimental Biology*, *211*, 3454–3466.

Broehan, G., Kroeger, T., Lorenzen, M., & Merzendorfer, H. (2013). Functional analysis of the ATP-binding cassette (ABC) transporter gene family of *Tribolium castaneum*. *BMC Genomics*, *14*, 6.

Campbell, J. L., & Nash, H. A. (2001). Volatile general anesthetics reveal a neurobiological role for the white and brown genes of *Drosophila melanogaster*. *Journal of Neurobiology*, *49*, 339–349.

Campesan, S., Green, E. W., Breda, C., Sathyasaikumar, K. V., Muchowski, P. J., Schwarcz, R., … Giorgini, F. (2011). The kynurenine pathway modulates neurodegeneration in a Drosophila model of Huntington's disease. *Current Biology*, *21*, 961–966.

de Castro, E., Sigrist, C. J. A., Gattiker, A., Bulliard, V., Langendijk-Genevaux, P. S., Gasteiger, E., … Hulo, N. (2006). ScanProsite: Detection of PROSITE signature matches and ProRule-associated functional and structural residues in proteins. *Nucleic Acids Research*, *34*, W362–W365.

Christie, A. E., Hull, J. J., Richer, J. A., Geib, S. M., & Tassone, E. E. (2017). Prediction of a peptidome for the western tarnished plant bug *Lygus hesperus*. *General and Comparative Endocrinology*, *243*, 22–38.

Coates, C. J., Jasinskiene, N., Miyashiro, L., & James, A. A. (1998). Mariner transposition and transformation of the yellow fever mosquito. *Aedes aegypti*. *Proceedings of the National Academy of Sciences of the United States of America*, *95*, 3748–3751.

Colinet, D., Kremmer, L., Lemauf, S., Rebuf, C., Gatti, J.-L., & Poirié, M. (2014). Development of RNAi in a Drosophila endoparasitoid wasp and demonstration of its efficiency in impairing venom protein production. *Journal of Insect Physiology*, *63*, 56–61.

Cornel, A. J., Benedict, M. Q., Rafferty, C., Howells, A. J., & Collins, F. H. (1997). Transient expression of the *Drosophila melanogaster* cinnabar gene rescues eye color in the white eye (WE) strain of *Aedes aegypti*. *Insect Biochemistry and Molecular Biology*, *27*, 993–997.

Debolt, J. W. (1982). Meridic diet for rearing successive generations of *Lygus hesperus*. *Annals of the Entomological Society of America*, *75*, 119–122.

Dong, Y., & Friedrich, M. (2005). Nymphal RNAi: Systemic RNAi mediated gene knockdown in juvenile grasshopper. *BMC Biotechnology*, *5*, 25.

Dow, J. A. T. (2001). *FlyBase error report for CG12286 and karmoisin on Thu Dec 6 07:17: 59 2001*. FlyBase.

Dreesen, T. D., Johnson, D. H., & Henikoff, S. (1988). The brown protein of *Drosophila melanogaster* is similar to the white protein and to components of active transport complexes. *Molecular and Cellular Biology*, *8*, 5206–5215.

Dustmann, J. H. (1968). Pigment studies on several eye-colour mutants of the honey bee. *Apis mellifera*. *Nature*, *219*, 950–952.

Edgar, R. C. (2004). MUSCLE: Multiple sequence alignment with high accuracy and high throughput. *Nucleic Acids Research*, *32*, 1792–1797.

Van Ekert, E., Wang, M., Miao, Y. G., Brent, C. S., & Hull, J. J. (2016). RNA interference-mediated knockdown of the Halloween gene *spookiest* (CYP307B1) impedes adult eclosion in the western tarnished plant bug, *Lygus hesperus*. *Insect Molecular Biology*, *25*, 550–565.

Ewart, G. D., Cannell, D., Cox, G. B., & Howells, A. J. (1994). Mutational analysis of the traffic ATPase (ABC) transporters involved in uptake of eye pigment precursors in *Drosophila melanogaster*. Implications for structure-function relationships. *The Journal of Biological Chemistry*, *269*, 10370–10377.

Fabrick, J. A., Kanost, M. R., & Baker, J. E. (2004). RNAi-induced silencing of embryonic tryptophan oxygenase in the Pyralid moth. *Plodia interpunctella*. *Journal of Insect Science*, *4*, 15.

Ferreiro, M. J., Pérez, C., Marchesano, M., Ruiz, S., Caputi, A., Aguilera, P., … Cantera, R. (2018). *Drosophila melanogaster* white mutant w1118 undergo retinal degeneration. *Frontiers in Neuroscience*, *11*, 435.

Finn, R. D., Clements, J., & Eddy, S. R. (2011). HMMER web server: Interactive sequence similarity searching. *Nucleic Acids Research*, *39*, W29–W37.

Fridell, Y. W. C., & Searles, L. L. (1991). Vermilion as a small selectable marker gene for Drosophila transformation. *Nucleic Acids Research*, *19*, 5082–5082.

Grubbs, N., Haas, S., Beeman, R. W., & Lorenzen, M. D. (2015). The ABCs of eye color in *Tribolium castaneum*: Orthologs of the Drosophila white, scarlet, and brown genes. *Genetics*, *199*, 749–759.

Hagler, J. (2009). Comparative studies of predation among feral, commercially-purchased, and laboratory-reared predators. *BioControl*, *54*, 351–361.

Halestrap, A. P. (2012). The monocarboxylate transporter family—Structure and functional characterization. *IUBMB Life*, *64*, 1–9.

Han, Q., Beerntsen, B. T., & Li, J. (2007). The tryptophan oxidation pathway in mosquitoes with emphasis on xanthurenic acid biosynthesis. *Journal of Insect Physiology*, *53*, 254–263.

Harris, D. A., Kim, K., Nakahara, K., Vásquez-Doorman, C., & Carthew, R. W. (2011). Cargo sorting to lysosome-related organelles regulates siRNA-mediated gene silencing. *The Journal of Cell Biology*, *194*, 77–87.

Hull, J. J., Chaney, K., Geib, S. M., Fabrick, J. A., Brent, C. S., Walsh, D., & Lavine, L. C. (2014). Transcriptome-based identification of ABC transporters in the western tarnished plant bug *Lygus hesperus*. *PLOS One*, *9*, e113046.

Hull, J. J., Geib, S. M., Fabrick, J. A., & Brent, C. S. (2013). Sequencing and de novo assembly of the western tarnished plant bug (*Lygus hesperus*) transcriptome. *PLOS One*, *8*, e55105.

Insausti, T. C., Le gall, M., & Lazzari, C. R. (2013). Oxidative stress, photodamage and the role of screening pigments in insect eyes. *The Journal of Experimental Biology*, *216*, 3200–3207.

Ishii, T. (1966). Some hereditary and ecological observations on small brown planthopper, *Laodelphax striatellus* (Fallén), having red-colored eye. *Japanese Journal of Applied Entomology and Zoology*, *10*, 64–68.

Jairin, J., Leelagud, P., Pongmee, A., & Srivilai, K. (2017). Chromosomal location of a recessive red-eye mutant gene in the brown planthopper *Nilaparvata lugens* (Stal) (Insecta: Hemiptera). *Advances in Entomology*, *5*, 33–39.

Jiang, Y., & Lin, X. (2018). Role of ABC transporters White, Scarlet and Brown in brown planthopper eye pigmentation. *Comparative Biochemistry and Physiology Part B, Biochemistry & Molecular Biology*, *221-222*, 1–10.

Kearse, M., Moir, R., Wilson, A., Stones-Havas, S., Cheung, M., Sturrock, S., … Drummond, A. (2012). Geneious Basic: An integrated and extendable desktop software platform for the organization and analysis of sequence data. *Bioinformatics*, *28*, 1647–1649.

Khan, S. A., Reichelt, M., & Heckel, D. G. (2016). Functional analysis of the ABCs of eye color in *Helicoverpa armigera* with CRISPR/Cas9-induced mutations. *Scientific Reports*, *7*, 40025.

Khanh, H. D. T., Bressac, C., & Chevrier, C. (2005). Male sperm donation consequences in single and double matings in *Anisopteromalus calandrae*. *Physiological Entomology*, *30*, 29–35.

Krstic, D., Boll, W., & Noll, M. (2013). Influence of the White locus on the courtship behavior of Drosophila males. *PLOS One*, *8*, e77904.

Kumar, S., Stecher, G., Li, M., Knyaz, C., & Tamura, K. (2018). MEGA X: Molecular Evolutionary Genetics Analysis across computing platforms. *Molecular Biology and Evolution*, *35*, 1547–1549.

Kômoto, N., Quan, G.-X., Sezutsu, H., & Tamura, T. (2009). A single-base deletion in an ABC transporter gene causes white eyes, white eggs, and translucent larval skin in the silkworm w-3oe mutant. *Insect Biochemistry and Molecular Biology*, *39*, 152–156.

Lawrence, P. A. (1970). Some new mutants of the large milkweed bug *Oncopeltus fasciatus* Dall. *Genetical Research*, *15*, 347–350.

Le, S. , Q., & Gascuel, O. (2008). An improved general amino acid replacement matrix. *Molecular Biology and Evolution*, *25*, 1307–1320.

Li, F., & Scott, M. J. (2016). CRISPR/Cas9-mediated mutagenesis of the white and sex lethal loci in the invasive pest, *Drosophila suzukii*. *Biochemical and Biophysical Research Communications*, *469*, 911–916.

Li, M., Au, L. Y. C., Douglah, D., Chong, A., White, B. J., Ferree, P. M., & Akbari, O. S. (2017). Generation of heritable germline mutations in the jewel wasp *Nasonia vitripennis* using CRISPR/Cas9. *Scientific Reports*, *7*, 901.

Liu, S.-H., Luo, J., Yang, B.-J., Wang, A. Y., & Tang, J. (2017). *karmoisin* and *cardinal* ortholog genes participate in the ommochrome synthesis of *Nilaparvata lugens* (Hemiptera: Delphacidae). *Insect Science*, 1–28.

Liu, S.-H., Wang, A. Y., Yang, B.-J., Luo, J., & Tang, J. (2017). Knockdown of an ABC transporter leads to bright red eyes in the brown planthopper, *Nilaparvata lugens* (Stål) (Hemiptera: Delphacidae). *Journal of Asia-Pacific Entomology*, *20*, 421–428.

Liu, S.-H., Yang, B.-J., Wang, A. Y., Luo, J., & Tang, J. (2018). The white gene in *Nilaparvata lugens* and its expression pattern under two different survival stresses. *Journal of Asia-Pacific Entomology*, *21*, 701–707.

Liu, S.-H., Yao, J., Yao, H.-W., Jiang, P.-L., Yang, B.-J., & Tang, J. (2013). Biological and biochemical characterization of a red-eye mutant in *Nilaparvata lugens* (Hemiptera: Delphacidae). *Insect Science*, *21*, 469–476.

Lloyd, V., Ramaswami, M., & Krämer, H. (1998). Not just pretty eyes: Drosophila eye-colour mutations and lysosomal delivery. *Trends in Cell Biology*, *8*, 257–259.

Lorenzen, M. D., Brown, S. J., Denell, R. E., & Beeman, R. W. (2002). Cloning and characterization of the *Tribolium castaneum* eye-color genes encoding tryptophan oxygenase and kynurenine 3-monooxygenase. *Genetics*, *160*, 225–234.

Loukeris, T. G., Livadaras, I., Arc , B., Zabalou, S., & Savakis, C. (1995). Gene transfer into the medfly, *Ceratitis capitata*, with a *Drosophila hydei* transposable element. *Science*, *270*, 2002–2005.

Mackenzie, S. M., Brooker, M. R., Gill, T. R., Cox, G. B., Howells, A. J., & Ewart, G. D. (1999). Mutations in the white gene of *Drosophila melanogaster* affecting ABC transporters that determine eye colouration. *Biochimica et Biophysica Acta*, *1419*, 173–185.

Mackenzie, S. M., Howells, A. J., Cox, G. B., & Ewart, G. D. (2000). Sub-cellular localisation of the White/Scarlet ABC transporter to pigment granule membranes within the compound eye of *Drosophila melanogaster*. *Genetica*, *108*, 239–252.

Mochida, O. (1970). A red-eyed form of the brown planthopper, *Nilaparvata lugens* (Stål)(Hom., Auchenorrhyncha). *Bulletin of the Kyushu Agricultural Experiment Station*, *15*, 141–273.

Moraes, A. S., Pimentel, E. R., Rodrigues, V. L. C. C., & Mello, M. L. S. (2005). Eye pigments of the blood-sucking insect, *Triatoma infestans* Klug (Hemiptera, Reduviidae). *Brazilian Journal of Biology*, *65*, 477–481.

Naranjo, S. E., Ellsworth, P. C., & Dierig, D. A. (2011). Impact of *Lygus* spp. (Hemiptera: Miridae) on damage, yield and quality of lesquerella (*Physaria fendleri*), a potential new oil-seed crop. *Journal of Economic Entomology*, *104*, 1575–1583.

Navrotskaya, V., & Oxenkrug, G. (2016). Effect of kynurenic acid on development and aging in wild type and vermilion mutants of *Drosophila melanogaster*. *Pharmacology, Drug Development & Therapeutics*, 1.

Osanai-Futahashi, M., Tatematsu, K., Futahashi, R., Narukawa, J., Takasu, Y., Kayukawa, T., … Sezutsu, H. (2015). Positional cloning of a Bombyx pink-eyed white egg locus reveals the major role of cardinal in ommochrome synthesis. *Heredity*, *116*, 135–145.

Osanai-Futahashi, M., Tatematsu, K., Yamamoto, K., Narukawa, J., Uchino, K., Kayukawa, T., … Sezutsu, H. (2012). Identification of the Bombyx red egg gene reveals involvement of a novel transporter family gene in late steps of the insect ommochrome biosynthesis pathway. *The Journal of Biological Chemistry*, *287*, 17706–17714.

Oxenkrug, G. F. (2010). The extended life span of *Drosophila melanogaster* eye-color (white and vermilion) mutants with impaired formation of kynurenine. *Journal of Neural Transmission*, *117*, 23–26.

Patana, R. (1982). Disposable diet packet for feeding and oviposition of *Lygus hesperus* (Hemiptera: Miridae). *Journal of Economic Entomology*, *75*, 668–669.

Perera, O. P., Little, N. S., & Pierce, C. A. (2018). CRISPR/Cas9 mediated high efficiency knockout of the eye color gene Vermillion in *Helicoverpa zea* (Boddie). *PLOS One*, *13*, e0197567.

Pires, H. H. R., Abrão, D. O., Machado, E. M. M., Schofield, C. J., & Diotaiuti, L. (2002). Eye colour as a genetic marker for fertility and fecundity of *Triatoma infestans* (Klug, 1834) Hemiptera, Reduviidae, Triatominae. *Memorias do Instituto Oswaldo Cruz*, *97*, 675–678.

Quan, G. X., Kim, I., Kômoto, N., Sezutsu, H., Ote, M., Shimada, T., … Tamura, T. (2002). Characterization of the kynurenine 3-monooxygenase gene corresponding to the white egg 1 mutant in the silkworm *Bombyx mori*. *Molecular Genetics and Genomics*, *267*, 1–9.

Reed, R. D., & Nagy, L. M. (2005). Evolutionary redeployment of a biosynthetic module: Expression of eye pigment genes vermilion, cinnabar, and white in butterfly wing development. *Evolution & Development*, *7*, 301–311.

Ritter, R. A., Lenssen, A. W., Blodgett, S. L., & Taper, M. L. (2010). Regional assemblages of *Lygus* (Heteroptera: Miridae) in Montana canola fields. *Journal of the Kansas Entomological Society*, *83*, 297–305.

Savvateeva, E., Popov, A., Kamyshev, N., Bragina, J., Heisenberg, M., Senitz, D., … Riederer, P. (2000). Age-dependent memory loss, synaptic pathology and altered brain plasticity in the Drosophila mutant cardinal accumulating 3-hydroxykynurenine. *Journal of Neural Transmission*, *107*, 581–601.

Schindelin, J., Arganda-Carreras, I., Frise, E., Kaynig, V., Longair, M., Pietzsch, T., … Cardona, A. (2012). Fiji: An open-source platform for biological-image analysis. *Nature Methods*, *9*, 676–682.

Schwartz, M. D., & Foottit, R. (1998). *Revision of the Nearctic species of the genus Lygus Hahn, with a review of the Palaearctic species (Heteroptera: Miridae)*. Memoirs on Entomology 10. Gainesville, Florid, International Associated Publishers.

Scott, D. R. (1977). An annotated listing of host plants of *Lygus hesperus* Knight. *Bulletin of the Entomological Society America*, *23*, 19–22.

Searles, L. L., & Voelker, R. A. (1986). Molecular characterization of the Drosophila vermilion locus and its suppressible alleles. *Proceedings of the National Academy of Sciences of the United States of America*, *83*, 404–408.

Seo, B. Y., Jung, J. K., & Kim, Y. (2011). An orange-eye mutant of the brown planthopper, *Nilaparvata lugens* (Hemiptera: Delphacidae). *Journal of Asia-Pacific Entomology*, *14*, 469–472.

Sethuraman, N., & O'Brochta, D. A. (2005). The *Drosophila melanogaster* cinnabar gene is a cell autonomous genetic marker in *Aedes aegypti* (Diptera: Culicidae). *Journal of Medical Entomology*, *42*, 716–718.

Shimizu, T., & Kawasaki, K. (2001). Red-eye mutants in Orius bugs (Heteroptera: Anthocoridae). *Applied Entomology and Zoology*, *36*, 185–187.

Shukle, R. H., Yoshiyama, M., Morton, P. K., Johnson, A. J., & Schemerhorn, B. J. (2008). Tissue and developmental expression of a gene from Hessian fly encoding an ABC-active-transporter protein: Implications for Malpighian tubule function during interactions with wheat. *Journal of Insect Physiology*, *54*, 146–154.

Sigrist, C. J. A., Cerutti, L., de Castro, E., Langendijk-Genevaux, P. S., Bulliard, V., Bairoch, A., & Hulo, N. (2010). PROSITE, a protein domain database for functional characterization and annotation. *Nucleic Acids Research*, *38*, D161–D166.

Slaymaker, P. H., & Tugwell, N. P. (1984). Inheritance of red eye color in *Lygus lineolaris* (Palisot de Beauvois) (Hemiptera: Miridae), an abnormal trait. *Journal of the Kansas Entomological Society*, *57*, 343–344.

Snodgrass, G. L. (2002). Characteristics of a red-eye mutant of the tarnished plant bug (Heteroptera: Miridae). *Annals of the Entomological Society of America*, *95*, 366–369.

Strand, L. L. (2008). *Integrated pest management for strawberries* (2nd ed., Vol. 3351*). Oakland, CA: Agriculture and Natural Resources, University of California.*

Summers, K. M., Howells, A. J., & Pyliotis, N. A. (1982). Biology of eye pigmentation. *Advances in Insect Physiology*, *16*, 119–166.

Tassone, E. E., Geib, S. M., Hall, B., Fabrick, J. A., Brent, C. S., & Hull, J. J. (2016). De novo construction of an expanded transcriptome assembly for the western tarnished plant bug. *Lygus hesperus*. *GigaScience*, *5*, 6.

Tatematsu, K., Yamamoto, K., Uchino, K., Narukawa, J., Iizuka, T., Banno, Y., … Daimon, T. (2011). Positional cloning of silkworm white egg 2 (w-2) locus shows functional conservation and diversification of ABC transporters for pigmentation in insects. *Genes to Cells*, *16*, 331–342.

Tearle, R. (1991). Tissue specific effects of ommochrome pathway mutations in *Drosophila melanogaster*. *Genetical Research*, *57*, 257–266.

Tsuji, T., Gotoh, H., Morita, S., Hirata, J., Minakuchi, Y., Yaginuma, T., … Niimi, T. (2018). Molecular characterization of eye pigmentation-related ABC transporter genes in the ladybird beetle *Harmonia axyridis* reveals striking gene duplication of the *white* gene. *Zoological Science*, *35*, 260–267.

Walker, A. R., Howells, A. J., & Tearle, R. G. (1986). Cloning and characterization of the vermilion gene of *Drosophila melanogaster*. *Molecular and General Genetics*, *202*, 102–107.

Wang, L., Kiuchi, T., Fujii, T., Daimon, T., Li, M., Banno, Y., … Shimada, T. (2013). Mutation of a novel ABC transporter gene is responsible for the failure to incorporate uric acid in the epidermis of ok mutants of the silkworm, *Bombyx mori*. *Insect Biochemistry and Molecular Biology*, *43*, 562–571.

Wang, L. H., Zhuang, Z., Li, Y., & Fang, J. (2013). Biological characteristics and mating advantage of the red-eye mutant of the small brown planthopper, *Laodelphax striatellus* (Hemiptera: Delphacidae). *Acta Entomologica Sinica*, *56*, 878–883.

Warren, W. D., Palmer, S., & Howells, A. J. (1996). Molecular characterization of the cinnabar region of *Drosophila melanogaster*: Identification of the cinnabar transcription unit. *Genetica*, *98*, 249–262.

Wheeler, A. G. (2001). *Biology of the plant bugs (Hemiptera: Miridae): Pests, predators, opportunists.* Ithaca, NY: Comstock Publishing Associates.

White, L. D., Coates, C. J., Atkinson, P. W., & O'Brochta, D. A. (1996). An eye color gene for the detection of transgenic non-drosophilid insects. *Insect Biochemistry and Molecular Biology*, *26*, 641–644.

Wilkens, S. (2015). Structure and mechanism of ABC transporters. *F1000Prime Reports*, *7*, 14.

Xiao, C., & Robertson, R. M. (2016). Timing of locomotor recovery from anoxia modulated by the white gene in Drosophila. *Genetics*, *203*, 787–797.

Xue, W.-H., Xu, N., Yuan, X.-B., Chen, H.-H., Zhang, J.-L., Fu, S.-J., … Xu, H. J. (2018). CRISPR/Cas9-mediated knockout of two eye pigmentation genes in the brown planthopper, *Nilaparvata lugens* (Hemiptera: Delphacidae). *Insect Biochemistry and Molecular Biology*, *93*, 19–26.

Zhang, H., Kiuchi, T., Hirayama, C., Katsuma, S., & Shimada, T. (2018). Bombyx ortholog of the Drosophila eye color gene brown controls riboflavin transport in Malpighian tubules. *Insect Biochemistry and Molecular Biology*, *92*, 65–72.

Zwiebel, L. J., Saccone, G., Zacharopoulou, A., Besansky, N. J., Favia, G., Collins, F. H., … afatos, F. C. (1995). The white gene of *Ceratitis capitata*: A phenotypic marker for germline transformation. *Science*, *270*, 2005–2008.

SUPPORTING INFORMATION

Additional supporting information may be found online in the Supporting Information section at the end of the article.

How to cite this article: Brent CS and Hull JJ. RNA interference-mediated knockdown of eye coloration genes in the western tarnished plant bug (*Lygus hesperus* Knight). *Arch. Insect Biochem. Physiol.* 2019;100: e21527. https://doi.org/10.1002/arch.21527